

ACCEPTED MANUSCRIPT

This is an early electronic version of an as-received manuscript that has been accepted for publication in the Journal of the Serbian Chemical Society but has not yet been subjected to the editing process and publishing procedure applied by the JSCS Editorial Office.

Please cite this article as K. A. Aliyev, S. O. Mammadova, A. N. Sultanova, Ahmad I. Ahmadov, I. Z. Sardarova, and A. N. Gurbanov, *J. Serb. Chem. Soc.* (2026) <https://doi.org/10.2298/JSC251120026A>

This “raw” version of the manuscript is being provided to the authors and readers for their technical service. It must be stressed that the manuscript still has to be subjected to copyediting, typesetting, English grammar and syntax corrections, professional editing and authors’ review of the galley proof before it is published in its final form. Please note that during these publishing processes, many errors may emerge which could affect the final content of the manuscript and all legal disclaimers applied according to the policies of the Journal.



J. Serb. Chem. Soc. **00(0)** 1-10 (2026)
JSCS-13641

The features of the intrinsic photoconductivity spectra of silver-doped zinc sulphide

KAZIM A. ALIYEV¹, SAADAT O. MAMMADOVA¹, AYTAN N. SULTANOVA^{1*},
AHMAD I. AHMADOV¹, ICABIKA Z. SARDAROVA², ABDULAGA N. GURBANOV^{2†}

¹Baku State University, Baku, Azerbaijan, and ²Azerbaijan State Oil and Industry University, Baku, Azerbaijan.

(Received 20 November 2025; revised 30 January 2026; accepted 13 May 2026)

Abstract: The intrinsic photoconductivity of silver-doped zinc sulphide (ZnS:Ag) was investigated. It was shown that doping with silver leads to significant modifications in the electronic structure and optical properties of ZnS due to the formation of localized energy levels within the band gap. Mechanical polishing of the sample surface results in the appearance of an additional photoconductivity maximum near the fundamental absorption edge, which gradually disappears during sample aging. These effects are attributed to the compensation of donor and acceptor states, as well as changes in charge carrier recombination mechanisms. The dependence of the photoconductivity spectrum on aging time, applied electric field, and the position of illumination relative to the contacts was established. The results are explained by variations in the lifetime of non-equilibrium charge carriers with depth. A qualitative model describing the photoconductivity spectra is proposed, taking into account the influence of silver compensation on the energy structure of ZnS. The proposed model provides insight into photoconductive mechanisms and supports the development of ZnS-based optoelectronic materials.

Keywords: photoconductivity spectra; absorption coefficient; optoelectronic material.

INTRODUCTION

The great importance of modern research on photoconductivity has been the recent rapid growth of interest in all areas of solid state physics and chemistry.¹⁻⁵ Alloying of silver in single crystals leads to their significant compensation and results in their high sensitivity to radiation.⁶⁻¹⁰

The main interest in ZnS:Ag is due to the fact that its photoconductivity excitation spectrum coincides with the emission spectrum of serial GaAs-based LEDs, which allows ZnS to be considered as a promising material for the

* Corresponding authors. E-mails: * aytansultanova@bsu.edu.az ; † qabdulaga@mail.ru
<https://doi.org/10.2298/JSC251120026A>

manufacture of high-performance resistor opt couplers.¹¹⁻¹⁸ The reasons for the high photosensitivity of ZnS:Ag and CdS:Ag samples are not fully understood, but there is evidence of the presence of two levels of semiconductor sulphides in forbidden gap, spaced 0.3 eV apart¹²⁻¹⁷ and located above top of the valence band.¹⁹⁻²¹ The authors explored the idea of a possible relation between the indicated levels and the localization features of silver in the ZnS lattice to explain the reason for the appearance of an additional photoconductivity maximum in the samples in the region of the fundamental absorption edge.²²⁻²⁴ It is assumed that silver impurities exhibit similar behavior in the investigated semiconductor sulphides.²⁵⁻³⁰

EXPERIMENTAL

For alloying silver, zinc sulphide grown by the Czochralski method with an electron concentration of $9.2 \cdot 10^{14} \text{ cm}^{-3}$ was used. Diffuse saturation of silver was carried out from a silver film sawed onto both surfaces in vacuum-sealed quart ampoules evacuated to 10^{-5} Torr at temperatures of 800-900 °C. Diffusion time 1-10 hours. After annealing, the ampoules were quenched in cold water, the samples were ground with abrasive powders and polished with diamond paste. Hall effect measurements of free charge carrier concentration in annealed samples indicate that alloying enables the formation of both high-resistivity ($n = 2.4 \times 10^8 - 10^9 \text{ cm}^{-3}$) and low-resistivity ($n = 1.4 \times 10^{15} \text{ cm}^{-3}$) materials. Contacts made of liquid eutectic Zn, Cd were applied to the polished surface of the samples in the form of two parallel strips, 2.2-3 mm long, with a gap between them. The photoconductivity signal was measured in the constant field mode using the modulation technique with synchronous detection at a modulation frequency of 8-400 Hz. For the study, high-quality samples were used to achieve a photocurrent that significantly exceeds the dark current when illuminated.

RESULTS AND DISCUSSION

Immediately after mechanical polishing of the sample surface, the photoconductivity spectrum exhibits two distinct maxima in the region of the fundamental absorption edge (Fig. 1). The short-wavelength maximum gradually disappears during storage under ambient conditions and is no longer observed after approximately two days. A similar effect is observed after thermal annealing, indicating that the additional peak is associated with surface-related states.

The figure 2 shows the spectral dependence of the photoconductivity of Ag-doped ZnS single crystals as a function of photon energy in the region close to the fundamental absorption edge.

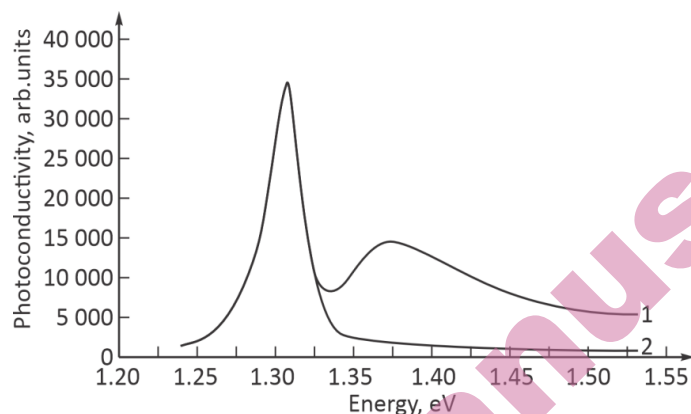


Fig 1. Photoconductivity spectrum of ZnS:Ag immediately after polishing and after two days. Experimental data; 1 - after polishing at 250 V; 2 - after 50 hours at a voltage of 250 V

Figure 2 shows the photoconductivity spectra for 60 V and 450 V.

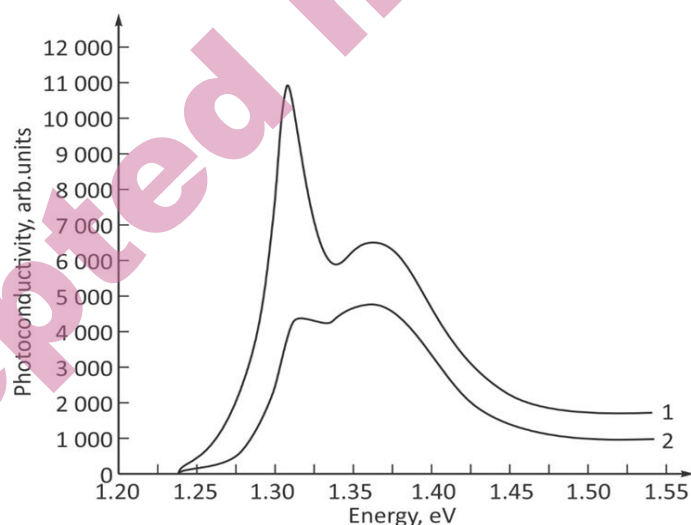


Fig. 2. Photoconductivity spectrum of ZnS:Ag a polished sample at different voltages. Experimental data at 1 – 60 V, 2 – 450 V

As seen from the spectra, the photoconductivity begins to increase rapidly when the photon energy approaches the fundamental absorption edge of ZnS. This behavior is associated with the generation of electron-hole pairs due to interband optical transitions. A pronounced maximum is observed in the short-wavelength region near approximately 1.30–1.32 eV. This peak can be attributed to intrinsic photoconductivity related to electronic transitions involving defect levels or localized states in the band gap introduced by silver doping. Two curves are

presented in the figure 2, corresponding to different surface conditions of the sample. Curve 1 exhibits a significantly higher photoconductivity signal compared to curve 2. This difference indicates that surface treatment strongly affects the photoconductive response of the crystal. Mechanical polishing modifies the surface defect structure and may create additional surface states that participate in charge carrier generation or recombination processes. After the main maximum, the photoconductivity gradually decreases with increasing photon energy. This behavior can be explained by changes in the efficiency of carrier generation, recombination processes, and carrier transport in the crystal. Overall, the observed spectral features demonstrate that both bulk defect states and surface-related states contribute to the formation of the intrinsic photoconductivity spectra in Ag-doped ZnS crystals. The results confirm that surface conditions play an important role in determining the magnitude and shape of the photoconductivity response.

It was noted that when focusing the beam near the negative contact, the short-wave peak predominated, and near the positive contact, the long-wave peak predominated (Fig. 3). The interval between the start of two experiments was no more than 10 minutes.

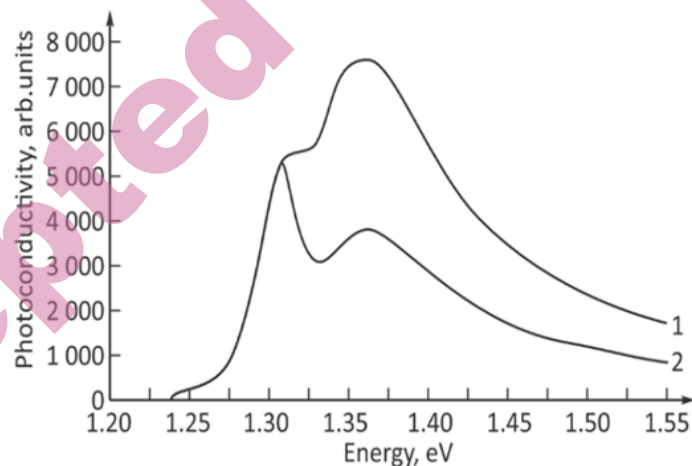


Fig. 3. Photoconductivity spectrum of a ZnS:Ag sample immediately after polishing with the focussing beam near the positive and negative contacts at a voltage of 200 V. Experimental data for field focusing 1 - near the negative contact, 2 - near the positive contact.

Previously, the observation of additional extrema beyond the fundamental absorption band edge in the ZnS:Ag photoconductivity spectra was explained.²

Let's consider a sample model consisting of several layers. We assume that in ZnS:Ag the quantum yield η is constant in each layer, and the change in mobility from layer to layer is small.² Then the photoconductivity $\Delta\sigma$ of the entire sample can be described by the following equation:

$$\Delta\sigma(h\nu) = Q_1[1 - \exp(-at_1)] + Q_2 \exp(-at_1) \times [1 - \exp(-at_2)] + Q_3 \exp(-at_1) \exp(-at_2) [1 - \exp(-at_3)] + Q_4 \exp(-at_1) \exp(-at_2) \exp(-at_3) \cdot 1 - \exp[\alpha(d - t_1 - t_2 - t_3)] \quad (1)$$

Where Q is the coefficient proportional to the lifetime for each layer; $\alpha = f(h\nu)$ is the performance dependence of the absorption coefficient of ZnS; t_1 is the layer thickness; d is the sample thickness. Q_1 characterizes the contribution of fast recombination processes occurring in the near-surface layer of the crystal. Q_2 describes the trapping and recombination of charge carriers through localized states associated with surface defects. Q_3 represents the contribution of recombination processes occurring in the bulk region of the crystal. Q_4 characterizes the transport of photogenerated charge carriers into deeper layers of the crystal and delayed recombination processes. These parameters are used to fit the shape of the photoconductivity spectra and make it possible to evaluate the relative influence of different recombination mechanisms.

The absorption coefficient α of zinc sulphide was measured by us independently and the result presented in Fig. 4 is in good agreement with the data.³ Regions of weak and strong absorption were approximated. In the region of fundamental absorption, as the energy of light quanta increases, the absorption coefficient increases significantly, which leads to a decrease in the penetration depth of light. For the energy range from 1.20 to 1.50 eV, the sample can be conditionally divided into 4 layers.

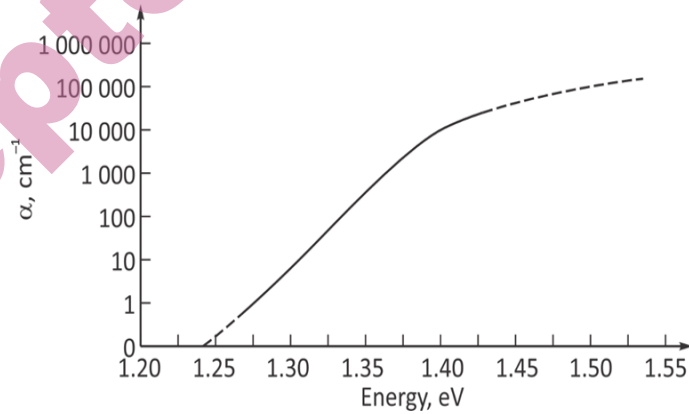


Fig. 4. Spectral dependence of the absorption coefficient of zinc sulphide.

Expression (1) described the photoconductivity spectra after polishing for holding times from 0 to 50 hours. The standard deviation did not exceed $4.285 \cdot 10^{-3}$. The values of the obtained parameters of equation (1) are given in Table I.

TABLE I Measurement Data for Q-Parameters and Thickness Values t_1-t_4

t_1-t_4	Q_1	Q_2	Q_3	Q_4	$t_1, \mu\text{m}$	$t_2, \mu\text{m}$	$t_3, \mu\text{m}$	$t_4, \mu\text{m}$	$d, \mu\text{m}$
0	4720	14845	2788	50820	0,1843	20,05	205,1	1508,7	1675
1	3790	11440	2885	51840	0,1948	21,06	210,8	1539,8	1675
2	2880	10032	2886	51841	0,1946	21,07	210,7	1542,2	1675
3	2390	8195	2877	51846	0,1947	21,09	210,6	1543,1	1675
4	1880	6545	2881	51849	0,1942	21,02	210,5	1543,4	1675
5	1539	5895	2882	51852	0,1949	21,05	210,3	1544,5	1675
6	1440	5506	2875	51853	0,1943	21,04	210,2	1543,6	1675
7	1180	5356	2873	51854	0,1944	21,06	210,7	1542,2	1675
24	580	3107	2871	51855	0,1946	21,07	210,9	1542,9	1675
47	280	1608	2882	51857	0,1942	21,08	210,4	1543,4	1675

When approximating the photoconductivity spectra at different voltages using equation (1) (Fig. 2), it was noted that with an increase in voltage from 60 to 450 V, the parameter Q_1 increased by 1.7 times, Q_2 and Q_3 by 1.3 times, and αQ_4 by 3 times. This means that with an increase in the electric field strength, the lifetime of carriers in the depth of the sample increases most of all. The thickness of the first layer increased by 2 times compared to the data in Table I, however, the thicknesses of the remaining layers did not change significantly. Table II shows the values of the parameters of equation (1) for approximating the photoconductivity spectra when focusing the beam near the negative (-) and positive (+) contacts (Fig. 3)

TABLE II Comparison of Positive and Negative Focusing on Q-Values and Layer Thicknesses

Focusing the meadow near the contact	Q_1	Q_2	Q_3	Q_4	$t_1, \mu\text{m}$	$t_2, \mu\text{m}$	$t_3, \mu\text{m}$	$t_4, \mu\text{m}$	$d, \mu\text{m}$
+	941	4034	1804	0,3938	0,3839	41,15	208,7	1524,6	1675
-	1850	7884	3803	5997	0,2852	61,05	210,8	1503,8	1675

The spectral characteristics of the intrinsic photoconductivity of silver-doped (ZnS:Ag) have been studied. It has been established that the presence of deep defect levels formed within the forbidden band of the crystal plays an important role. The compensation effect influences both the spectral sensitivity and the intensity of photoconductivity.

The photoconductivity mechanism in Ag-compensated ZnS crystals has a complex nature and is determined by the interaction between the band structure and defect-related states. The observed changes in the spectral response are associated with recombination processes involving deep levels. Similar effects have been reported in previous studies of ZnS-based materials, where defect states and surface conditions strongly influence carrier recombination and transport processes. Silver-doped ZnS materials are widely used in electroluminescent

panels, CRT phosphors, and UV detectors because of their favorable optical and electrical characteristics.

One of the main results of the present study is the appearance of an additional short-wavelength photoconductivity maximum near the fundamental absorption edge after mechanical polishing of the crystal surface. This observation indicates that surface treatment modifies the defect structure in the near-surface region and introduces additional localized states within the band gap. The gradual decrease in the intensity of this maximum with aging time suggests relaxation or recombination of the surface-related defect states.

The experimental results also show that increasing the applied electric field enhances the photoconductivity signal due to more effective separation and transport of photo-generated charge carriers. In addition, the photoconductivity spectra depend on the position of illumination relative to the electrical contacts, indicating the contribution of carrier injection processes. To explain the experimental observations, a multilayer phenomenological model was used, in which the crystal is considered as a system of layers with different recombination properties and carrier lifetimes. This approach makes it possible to describe the depth-dependent behavior of photo-generated carriers in the crystal.

CONCLUSION

The intrinsic photoconductivity spectra of Ag-compensated ZnS crystals exhibit characteristic features associated with electronic transitions near the fundamental absorption edge. In particular, an additional short-wavelength photoconductivity maximum appears after mechanical polishing of the sample surface. Similar surface-related effects have been reported in previous studies on ZnS-based materials, where surface treatment was shown to introduce localized states within the band gap and modify recombination processes.¹⁻³

The observed decrease in the intensity of this maximum with increasing aging time indicates relaxation of surface defect states. This behavior is in agreement with literature data, where the evolution of surface states and space charge regions has been shown to influence photoconductivity in II-VI semiconductors.^{2,4}

The experimental results also demonstrate that the photoconductivity depends on the applied electric field and the position of illumination relative to the contacts. The increase in photoconductivity with electric field strength can be attributed to enhanced separation of photogenerated carriers, which is consistent with previously reported results for ZnS and related compounds.^{3,5} In addition, the influence of carrier injection from contacts, leading to recharging of impurity centers, has also been discussed in earlier works.⁴

To interpret the experimental observations, a multilayer phenomenological model was applied, in which the crystal is considered as a system of layers with different carrier lifetimes. Such an approach allows one to take into account the

depth-dependent behavior of non-equilibrium carriers and the variation of the space charge region near the surface. Similar modeling approaches have been successfully used in the analysis of photoconductivity in compensated semiconductors.⁵

The appearance of the short-wavelength maximum can be attributed to mechanical stresses induced by surface polishing, as well as to the formation of a space charge region influenced by interaction with the ambient atmosphere. The variation of photoconductivity maxima with electric field strength and illumination geometry indicates that the lifetime of non-equilibrium carriers changes with depth, which is consistent with the proposed model.

ИЗВОД

КАРАКТЕРИСТИКЕ СПЕКТАРА СОПСТВЕНЕ ФОТОПРОВОДЉИВОСТИ ЦИНК-СУЛФИДА ДОПИРАНОГ СРЕБРОМ

KAZIM A. ALIYEV¹, SAADAT O. MAMMADOVA¹, AY TAN N. SULTANOVA^{1*}, ICABIKA Z. SARDAROVA², ABDULAGA N. GURBANOV^{2*}

¹Baku State University, Baku, Azerbaijan, and ²Azerbaijan State Oil and Industry University, Baku, Azerbaijan.

Испитивана је сопствена фотопроводљивост цинк сулфида допираног сребром (ZnS:Ag). Показано је да допирање сребром доводи до значајних модификација у електронској структури и оптичким својствима ZnS због формирања локализованих енергетских нивоа унутар забрањене зоне. Механичко полирање површине узорка резултира појавом додатног максимума фотопроводљивости близу фундаменталне ивице апсорпције, који постепено нестаје током старења узорка. Ови ефекти се приписују компензацији донорског и акцепторског стања, као и променама у механизмима рекомбинације носилаца наелектрисања. Утврђена је зависност спектра фотопроводљивости од времена старења, примењеног електричног поља и положаја осветљења у односу на контакте. Резултати се објашњавају варијацијама у животном веку неравнотежних носилаца наелектрисања са дужином. Предложен је квалитативни модел који описује спектре фотопроводљивости, узимајући у обзир утицај компензације сребра на енергетску структуру ZnS. Предложени модел пружа увид у фотопроводљиве механизме и подржава развој оптоелектронских материјала на бази ZnS.

(Примљено 20. новембра 2025; ревидирано 30. јануара 2026; прихваћено 13. маја 2026.)

REFERENCES

1. S.Thirumavalavan, K. Mani, S. Sagadevan, *Sci. Res. Essays* **10** (2015) 362 (<https://doi.org/10.5897/sre2015.6244>)
2. S.Jeong, S.Park, *App. Sci.* **12** (2022) 8393 (<https://doi.org/10.3390/app12178393>)
3. A. Bera, D. Basak D, *ACS App. Mat. Sci.* **2** (2012) 408 (<https://doi.org/10.1021/am900686c>)
4. C. Galassi, N. Lecis, *Energies* **16** (2023) 6409 (<https://doi.org/10.3390/en16176409>)
5. M. M. H. Farooqi, R. K. Srivastava, *Mat. Sci. Semicond. Process.* **20**(1) (2014) 61 (<https://dx.doi.org/10.1016/j.mssp.2013.12.028>)

6. R. Srivastava, N. Pandey, S. Mishra, *Mat. Sci. Semicond. Process.* **16**(6) (2013) 1659 (<https://dx.doi.org/10.1016/j.mssp.2013.06.009>)
7. A. K. Shahi, B. K. Pandey, S. C. Singh, R. Gopal, *J. Alloys Comp.* **588** (2014) 440 (<https://dx.doi.org/10.1016/j.jallcom.2013.11.056>)
8. A. Shahi, R. Shankar, B. Pandey, R. Gopal, *Mat. Res. Inn.* **28**(3) (2024) 184 (<https://dx.doi.org/10.1080/14328917.2023.2250625>)
9. Z. Zhang, K. Wang, K. Zheng, S. Deng, N. Xu, J. Chen, *ACS Photonics* **5**(10) (2018) 4147 (<https://dx.doi.org/10.1021/acsp Photonics.8b00949>)
10. R. Singh, N. Unnikrishnan, M. Matera, *J. Phys. Chem. Solids* **49**(1) (1988) 79 ([https://dx.doi.org/10.1016/0022-3697\(88\)90138-2](https://dx.doi.org/10.1016/0022-3697(88)90138-2))
11. J. Rufat, *J. Nanosci. Res. Rep.* **3** (2021) 1 ([https://dx.doi.org/10.47363/jnsrr/2021\(3\)128](https://dx.doi.org/10.47363/jnsrr/2021(3)128))
12. V. Porter, S. Geyer, J. Halpert, M. Kastner, M. Bawend, *J. Phys. Chem. C* **112** (2008) 2231 (<https://dx.doi.org/10.1021/jp710173q>)
13. M. Ahmad, K. Rasool, M. A. Rafiq, M. M. Hasan, *Appl. Phys. Lett.* **101** (2012) 223103 (<https://doi.org/10.1063/1.4768784>)
14. M. M. H. Farooqi, R. K. Srivastava, *J. Alloys Comp.* **691** (2017) 275 (<https://dx.doi.org/10.1016/j.jallcom.2016.08.245>)
15. N. Suganthi, K. Pushpanathan, *Int. J. Env. Sci. Tech.* **16**(7) (2019) 3375 (<https://dx.doi.org/10.1007/s13762-018-1811-y>)
16. N. Susha, K. Nandaakumar, S. S. Nair, *RSC Adv.* **8**(21) (2018) 11330 (<https://dx.doi.org/10.1039/c7ra13116j>)
17. K. O. Olumurewa, S. A. Adewinbi, A. A. Willoughby, M. A. Eleruja, *Phase Trans.* **95**(8-9) (2022) 567 (<https://dx.doi.org/10.1080/01411594.2022.2093199>)
18. G. Wary, M. Sarma, *Indian J. Pure Appl. Phys.* **54**(6) (2016) 379, ISSN 00195596
19. S. Bhushan, L. C. Giriya, *Photoconductivity of (ZnS, CdSe): Dy in Crystal Research and Technology Vol. 22 No 9*, H. Neel et al (Eds), De Gruyter (1987) (<https://dx.doi.org/10.1515/9783112485569-015>)
20. Z. Zhang, C. Chen Wang, S. Deng, J. Chen, *Adv. Mat. Interf.* **9**(9) (2022) 2102268 (<https://dx.doi.org/10.1002/admi.202102268>)
21. I. Uddin, *Adv. Nano Res.* **3**(1) (2020) 46 (<https://dx.doi.org/10.21467/anr.3.1.46-50>)
22. M. Freitag, T. Low, F. Xia, P. Avorius, *Nature Photonics* **7** (2013) 53 (<https://doi.org/10.1038/nphoton.2012.314>)
23. S. Hullavarad, N. Hullavarad, D. Look, B. Claffin, *Nanoscale Res. Lett.* **4** (2009) 1421 (<https://doi.org/10.1007/s11671-009-9414-7>)
24. E. R. Draper, L. J. Archibald, M. C. Nolan, R. Schweins, M. A. Zwijnenburg, S. Sproules, D. J. Adams, *ChemEurJ* **24** (2018) 4006 (<https://doi.org/10.1002/chem.201800201>)
25. A. Di Bartolomeo, A. Kumar, O. Durante, A. Sessa, E. Faella, L. Viscardi, K. Intonti, F. Giubileo, N. Martucciello, P. Romano, S. Sleziona, M. Schleberger, *Mat. Today Nano* **24** (2023) 100382 (<https://doi.org/10.1016/j.mtnano.2023.100382>)
26. M. Ibraheem, E. Verrelli, A. M. Adawi, J.-S. G. Bouillard, Mary O'Neill, *ACS Omega* **9** (2024) 10169 (<https://doi.org/10.1021/acsomega.3c06932>)
27. Ph. V. Makarenko, N. N. Pribylov, S. I. Rembeza, V. A. Mel'nik, *Semiconductors* **42** (2008) 528 (<https://link.springer.com/article/10.1134/S1063782608050072>)
28. D. Xue, Y. Zhang, W. Gong, Y. Yin, Z. Wang, L. Huang, L. Chi, *Sci. China Chem.* **65** (2022) 2567 (<https://doi.org/10.1007/s11426-022-1368-7>)

ALIYEV *et al.*

29. R. F. Babayeva, A. Sh. Abdinov, S. I. Amirova, N. A. Ragimova, E. A. Rasulov, *UNEC J. Eng. Appl. Sci.* **3(1)** (2023) 5 (<https://doi.org/10.61640/ujeas.2023.0501>)
30. A. M. El-Naggar, A. A. Albassam, G. L. Myronchuk, O. V. Zamuruyeva, I. V. Kityk, P. Rakus, O. V. Parasyuk, J. Jędryka, V. Pavlyuk, M. Piaseck, *Mat. Sci. Semicond. Process.* **86** (2018) 101 (<https://doi.org/10.1016/j.mssp.2018.06.019>).

Accepted manuscript